Published in final edited form as:
J Biomed Mater Res A. 2013 May ; 101(5): 1427–1436. doi:10.1002/jbm.a.34437.

Phase Composition Control of Calcium Phosphate Nanoparticles for Tunable Drug Delivery Kinetics and Treatment of Osteomyelitis. Part 2: Antibacterial and Osteoblastic Response

Vuk Uskoković and **Tejal A. Desai**
Therapeutic Micro and Nanotechnology Laboratory, Department of Bioengineering and Therapeutic Sciences, University of California, San Francisco

Abstract

Osteomyelitis has been traditionally treated by the combination of long-term antibiotic therapies and surgical removal of diseased tissue. The multifunctional material was developed in this study with the aim to improve this therapeutic approach by: (a) enabling locally delivered and sustained release of antibiotics at a tunable rate, so as to eliminate the need for repetitive administration of systemically distributed antibiotics; and (b) controllably dissolving itself, so as to promote natural remineralization of the portion of bone lost to disease. We report hereby on the effect of the previously synthesized calcium phosphates (CAPs) with tunable solubilities and drug release time scales on bacterial and osteoblastic cell cultures. All CAP powders exhibited satisfying antibacterial performance against *Staphylococcus aureus*, the main causative agent of osteomyelitis. Still, owing to its highest drug adsorption efficiency, the most bacteriostatically effective phase was amorphous CAP with the minimal inhibitory concentration of less than 1 mg/ml. At the same time, the positive cell response and osteogenic effect of the antibiotic-loaded CAP particles was confirmed *in vitro* for all the sparsely soluble CAP phases. Adsorption of the antibiotic onto CAP particles reversed the deleterious effect that the pure antibiotic exerted on the osteogenic activity of the osteoblastic cells. The simultaneous osteogenic and antimicrobial performance of the material developed in this study, altogether with its ability to exhibit sustained drug release, may favor its consideration as a material base for alternative therapeutic approaches to prolonged antibiotic administration and surgical debridement typically prescribed in the treatment of osteomyelitis.

Introduction

The prevalence of bone disease is expected to increase as the population ages.[1] The number of hip and knee replacement procedures performed in the US has, for example, doubled in the past decade, while the number of reported cases of bone infection accompanying those has been also steadily increasing in proportion with the number of surgeries performed.[2] The majority of bone diseases are, however, systemic in nature, e.g., osteoporosis, calling for similarly systemic approaches to their treatment. Other diseases, some of which are infectious, e.g., osteomyelitis, exhibit a pronounced local character and demand equally localized treatments to prevent their spreading and systemic deterioration of the skeletal support of the organism as a whole. Local surgical operations that involve permanent removal of the diseased tissue, long-term antibiotic therapies and occasional implantation of hard tissue substitutes are typically prescribed to treat bone infection.[3] To improve on this partly invasive approach that often leaves the postoperative patients even frailer than before the treatment, novel therapies for infectious hard tissue diseases are actively being sought.[4–8]

This study aims at improving this rather imperfect contemporary medical approach to treating osteomyelitis by developing materials able to: (a) deliver a localized and sustained flux of antibiotics so as to eliminate the need for their repetitive administration and systemic distribution in the body; and (b) promote natural remineralization of the portion of bone lost to disease through their osteogenic nature. Calcium phosphates present a natural choice for the drug delivery carrier in the treatment of osteomyelitis because they share the chemical composition with the inorganic component of bone[9]. In the first part of this study, we described the synthesis of five different calcium phosphate (CAP) phases that covered the full range of solubility products for CAPs, from the most soluble monocalcium phosphate (MCPM; pK_{sp} 1.14) to the least soluble hydroxyapatite (HAP; pK_{sp} 117.3) (Table 1). The release of physisorbed proteins or small organics used as model drugs was shown to be directly conditioned by the dissolution rate of the powder, allowing for simple, stoichiometry-controlled tunability of the drug release kinetics, ranging from 1–2 hours to 1–2 years. In this part, we report on the results of our looking at the effect of these different monophasic CAP nanopowders on bacterial and MC3T3-E1 osteoblastic cell cultures.

Experimental part

Preparation of CL-loaded CAPs

Loading of CAP powders with clindamycin phosphate (CL; *Tokyo Chemical Industry*) followed the identical approach as that reported in the first part of the study for BSA and fluorescein, the two model drugs used to investigate the release profiles of the carriers. Loading with CL was qualitatively confirmed using differential scanning calorimetry (DSC; *Calorimetry Sciences Corporation*).

Bacterial studies

A single colony of *Staphylococcus aureus* (ATCC 25923) cultured on a blood agar plate over 48 h was stabbed with a pipette tip, which was then placed in 5 ml of 37 mg/ml brain heart infusion (BHI) broth and kept on an incubator shaker (*Innova 44*) overnight at 37 °C and 225 rpm. The turbid broth was collected the following day and 8 nl of it was added to serially diluted samples containing different concentrations of CL in 1 ml of 37 mg/ml BHI broth, for the purpose of determining the minimal inhibitory concentration (MIC) and minimal bactericidal concentration (MBC) of the pure drug under the given analytical conditions. The given bacterial concentration (1:125,000 of 5 ml 37 mg/ml BHI broth inoculated overnight with a single bacterial colony) was found to be equal to the standard concentration of 10^5 bacteria per ml after comparing the optical density at $\lambda = 600$ nm of a range of serially diluted bacterial broths with 0.5 M McFarland solution (equivalent to approximately 10^8 bacteria per ml) prepared by mixing 1 % $BaCl_2$ solution and 1 % H_2SO_4 in the volume ratio of 1:200, respectively. The dilution yielding the same absorbance as that of 0.5 M McFarland solution was diluted 10^3 times to yield the standard bacterial concentration of 10^5 bacteria per ml. The series of samples was incubated overnight on the incubator shaker and analyzed the following day for their optical density at $\lambda = 600$ nm using a *Micropack DS-2000* UV/Vis/NIR spectrophotometer. The MIC was determined as the point of intersection of the resulting transmittance vs. [CL] curve and the transmittance of the bacterial broth at zero time point. To assess the antibacterial performance of the CAP particles, different amounts of CL-containing CAP powders, ranging from 1 – 50 mg were added to 1 ml of 37 mg/ml BHI broth containing 10^5 bacteria, incubated overnight on the incubator shaker and analyzed the following day for their optical density at $\lambda = 600$ nm.

Cell culture studies

Mouse calvarial preosteoblastic cell line, MC3T3-E1 subclone 4, was purchased from American Tissue Culture Collection (*ATCC*, Rockville, MD) and cultured in Alpha

Minimum Essential Medium (α-MEM; *Gibco*) supplemented with 10% fetal bovine serum (FBS, *Invitrogen*) and no ascorbic acid (AA). The medium was replaced every 48 h, and the cultures were incubated at 37 °C in a humidified atmosphere containing 5% CO_2. Every 7 days, the cells were detached from the surface of the 75 cm^2 cell culture flask (*Greiner Bio-One*) using 0.25 wt% trypsin, washed, centrifuged (1000 rpm×3 min), resuspended in 10 ml media and subcultured in 1:7 volume ratio. Cell passages 2 – 5 were used for the experiments reported hereby. In all experiments, the cells were seeded either in 96 well plates and 100 μl of media at a density of 10^4 cells per well or on glass cover slips placed in 24 well plates and 400 μl of media at a density of 6×10^4 cells per well. The cultures were regularly examined under an optical microscope to monitor growth and possible contamination. Near confluence, cells were treated with 2 mg/cm^2 of CAP/CL particles and 50 μg/ml AA as the mineralization inductor, and incubated for 7 – 10 days. Alpha-MEM supplemented with 50 μg/ml AA was replenished every 48 h. Cells incubated with pure CL were cultured in the same medium containing 100 μg/ml CL.

After the incubation period of 7 days, cells grown in 24 well plates were stained by adding 200 μl of 2 μM calcein AM and 4 μM ethidium homodimer-1 (EthD-1) in phosphate buffer saline (PBS) and incubating at 37 °C for 45 min (*Invitrogen* L-3224). Inverted cover slips containing cells and CAP/CL particles were then mounted on microscope slides wetted with 20 μl of the staining solution and sealed using nail polish. Immediately thereafter, the live/dead cell count was performed under an *Olympus BX60* optical microscope. Three hours after the staining, single plane images of the samples were collected on a confocal laser scanning microscope - C1si (UCSF Nikon Imaging Center) at 60× and 100× magnifications in oil. All the experiments were carried out in quadruplicates. Another staining procedure involved first fixing the cells for 15 min in 3.7 % paraformaldehyde. The cells were then washed with PBS 3×5 min and then with the blocking solution (PBT = 1 % Bovine Serum Albumin (BSA), 0.1 % Triton X-100 in PBS) 2×5 min. The cells were then blocked and permeabilized in PBT for 1 h, and then incubated in 20 μg/ml 4',6-diamidino-2-phenylindole dihydrochloride nuclear counterstain (DAPI, Invitrogen), 2 μM calcein AM as HAP/CL - staining compound, and 10 μg/ml phalloidin-tetramethylrhodamine (AlexaFluor 555, Invitrogen), all in PBT for 1 h and then washed with PBS 3×5 min. The cover slips containing the fixed and stained cells were mounted onto glass slides using hard set vectashield and nail polish and were subsequently imaged on a confocal laser scanning microscope - C1si (UCSF Nikon Imaging Center) at 100×magnification in oil.

Differentiation of MC3T3-E1 fibroblasts into osteoblast-like cells entails the formation of a mineralized extracellular collagen matrix and the expression of genes associated with the osteoblastic phenotype[11]. After the incubation period of 10 days, cell lysis, reverse transcription (*Bio-Rad*) and qPCR (*Applied Biosystems, StepONEPlus*) were performed using the Fast SYBR Green Cells-to-CT kit (*Ambion*) in accordance with the manufacturer's instructions. Each experiment was done in quadruplicates, while each experimental replica was analyzed for mRNA expression in triplicates (n = 4×3). The expressions of one housekeeping gene, β-actin (*ACTB*), and five osteogenic markers, mouse type I procollagen (*Col I*), alkaline phosphatase (*ALP*), osteocalcin (*BGLAP*), osteopontin (*BSP-1*) and *Runx2* were analyzed. The primer pair sequences used are given in the supplementary section. The real-time PCR results were analyzed using the ΔΔCt method[12] and all the data were normalized to *ACTB* expression levels.

Results and Discussion

Since osteomyelitis can be potentially caused by a variety of infective agents, CL, a wide-range antibiotic commonly prescribed to treat infections caused by an array of gram-positive and gram-negative bacteria, aerobic and anaerobic, as well as fungi and protozoa[13], was

chosen as a model antibiotic for this study. The most serious side effect of its usage is reduced diversity of the intestinal microbiota and acute pseudomembranous colitis.[14,15] The phosphate form of CL, its proactive form owing to higher permeability of the cell membrane, was used due to its higher adsorption capacity to CAP, as the result of Ca^{2+}-PO_4^{3-} interaction[16], as well as higher solubility in aqueous media. Antibiotics can be broadly classified to two categories[17]: concentration-effective and time-effective, with CL belonging to the second category. Whereas the effective application of concentration-dependent antibiotics depends on the ability to bring their concentration in the target area to 10 – 12 times the MIC in a short period of time, for CL as a time-dependent antimicrobial, a direct correlation exists between the duration of the antimicrobial concentration exceeding the MIC and the time that it takes to eradicate the pathogen, with the bactericidal effect being optimal at 4 – 5 times the MIC *in vitro*.[18] Finding ways to sustain the period during which the concentration of CL exceeds the MIC for the given bacterial population is thus of vital importance in making the therapies involving this antibiotic more effective. Assessment of the antibacterial performance of CL-loaded CAP powders of different phase composition has correspondingly presented a central subject of this study. To complement this evaluation of the effectiveness of CAP/CL powders in eradicating the pathological source of infection, studies were also carried out to assess their osteogenic effects on osteoblastic cells *in vitro*.

Pharmacokinetic performance of particles prepared in this work can be divided to the following kinetic factors: (1) release from the dosage form; (2) distribution to the site of action; and (3) reaction with the targeted biochemical species.[19] Since (2) is a very fast step because the particles are meant to be surgically implanted in the vicinity of inflammation, the slowest rate between (1) and (3) will kinetically determine the drug performance. These two factors were in this work first evaluated separately by (a) measuring the rate of release of the drug from the particles, and (b) determining the MIC of the pure drug. Only then were these two combined and looked at in couple. Since the contents of the bacteriostatic agents as low as 0.2 % were shown to be effective in treating dental infection, CL loading efficiency, presumably comparable to that of fluorescein, should not be a critical factor in ensuring the antimicrobial performance of CAP/CL particles.[20]

The limited burst release in the first 24 h exhibited by all CAP powders presents a vital precondition for their effective acting in a bacteriostatic or bactericidal manner. Initial deviations from zero-order kinetics, often considered undesirable when sustained drug delivery is performed to treat nonbacterial pathologies, are thus vital for suppressing bacterial infection by controlled delivery of antibiotics, as timely transcendence of the MIC is required to prevent the rise of resistance to the given antibiotic among the bacterial population.[21] Previous studies on the MIC of CL with respect to *S aureus* have shown that, depending on the bacterial strain, the MIC can lie anywhere between 1 and 500 μg/ml.[22] As shown in Fig.1a, extrapolation of the linear range of the curve that represents the optical density of BHI broths inoculated with the standard concentration of a single colony of *S aureus* (10^5 bacteria per ml) at $\lambda = 600$ nm as a function of the concentration of the drug indicates that any [CL] > 24 μg/ml suppresses the bacterial growth. At [CL] > 150 μg/ml, the plateau is reached on the given curve, suggesting that the latter is the minimal bactericidal concentration (MBC) for the actual conditions. As the latter was found to be more than 4 times higher than the MIC, CL can be in this case considered as a bacteriostat rather than a bactericide.[23]

The optical transparence at $\lambda = 600$ nm and visual appearance of BHI broths inoculated with *S aureus* and incubated overnight with different amounts of CL-containing CAP powders as a function of the concentration of the latter are shown in Figs.1b and S2, respectively. The graph demonstrates different MIC levels for different CAP powders, all of which lie below

that of 15 mg/ml for MCPM (Table 2). The addition of MCPM dropped the pH to below 6 and it has been previously shown that pH drop from 7.4 to 5.5 increases the MIC of CL with respect to *S aureus* 16-fold.[24] A similar effect was observed in this study: although CL itself is stable at low pH[25] and the CL content in MCPM/CL powder was determined using UV absorption to > 5 wt%, the effective [CL] equaled only 0.2 %. This effect is explained by the exceptional tolerance of *S aureus* to low pH[26] and the decreased activity of CL, alongside many other antibiotics, in acidic media.[27] The most effective antibacterial performance was exhibited by ACP powders, in which case less than 1 mg/ml was sufficient to prevent the bacterial growth. This is presumably due to their highest level of burst dissolution among all the CAP powders, directly relatable to the comparatively high rate of initial drug release. Coupled with the earlier observed small molecule drug release time scale of 1–2 months, closest to the duration of antibiotic therapy for bone infection, these results favor ACP for the medical application conceived hereby more than any other CAP phase. The observed lower MIC for CL-loaded HAP than that for DCPA, which degrades faster than HAP, can be explained by the higher Ca/P ratio of HAP (1.667) compared to that of DCPA (1). Since Ca^{2+} ions presumably present the main binding points for negatively charged CL (pK_a = 0.96 and 6.06)[28] on CAP surface, their deficiency may directly relate to lower drug binding affinity. The effect of decreased binding efficiency of other small organic drug molecules, including bisphosphonates, in direct proportion with Ca^{2+} deficiency in HAP was previously observed.[29]

Experiments involving incubation of CAP/CL particles in broths buffered with 50 mM Tris/HCl (pH 7.4) showed no significant change from the MIC values given in Table 2, indicating that the mild acidifying effect that the dissolution of all CAP powders except MCPM (typified by rather strong acidification of the medium) has on the solution does not play a role in promoting the bacterial growth. Conversely, the alkaline nature of HAP and, presumably, ACP should not be a crucial factor in contributing to inhibition of the bacterial proliferation. The antimicrobial performance is mainly controlled by the release of the antibiotic, which is, in turn, contingent upon the extent of dissolution of CAP powders and their efficiency in binding the drug by physical adsorption. In support of this statement, Fig. 2 demonstrates how the opacity of different CAP/CL powders decreases upon their incineration beyond the melting point of CL (180 °C) in direct proportion with the MIC of the powders: the higher the CL content, the lower the MIC. DSC diagrams of pure CL and a CAP/CL powder, displaying the endothermic peak corresponding to the melting point of CL[30], are shown in Fig.3. The melting peak of CL becomes broader, covering a wider range of temperatures when the drug is impregnated within the CAP powder, owing to its greater level of dispersion in comparison with a crystalline state it occupies in the pure form.

Controlled drug delivery by means of implantable nanoparticles has been shown to produce local concentrations of the released drug well beyond the MIC levels and is considered a more effective means of delivery compared to intravenous route for specific applications that include lowly vascular tissues, including those comprising bone.[31–34] Although CL resistance does occur in *S aureus*[35] as well as among patients with osteomyelitis and with prior antibiotics exposure[36], the antibacterial assessment reported hereby suggests that the application of antibiotic-loaded CAP particles analyzed would not be any more likely than the traditional therapy to result in spontaneous drug resistance during treatment.

Cell culture studies

Upon incubation with osteoblastic cells for up to 21 days, none of the CAP powders loaded with CL except MCPM/CL exhibited toxic effects on the cells. The percentage of dead cells was < 2 % for all CAP/CL powders except MCPM/CL, with no significant difference from the negative control. Cells incubated with MCPM were, however, fully rounded and dead at the time of their visualization (Fig.4a). Moreover, it was noticed earlier that acidification

that entails dissolution of MCPM/CL also increases the MIC of CL required to stop the bacterial growth. This relatively powerful acidic nature of the most soluble CAP powder, MCPM, may present a major obstacle to its *in vivo* application. However, if the medium was refreshed immediately upon the dissolution of the MCPM particles, 1–2 h after their addition, the viability of the cell population was preserved (Fig.4b), despite being significantly decreased (40 – 60 %). This observation provides hopes that the flow of body fluids to and from the area of surgical implantation may still prevent the detrimental effects of the very fast dissolution of MCPM, the most acidic CAP phase, *in vivo*.

The results of fluorescent staining of CAP/CL particles and osteoblastic cells shown in Figs. 5–6 demonstrate excellent cell adherence and spreading on CAP/CL particles of all sparsely soluble phases remnant in the system after 7 days of incubation: HAP, ACP and DCPA. The in-plane images in Fig.6 correspondingly display blue-stained cell nuclei elongated in the direction of the particle surface, with red-stained f-actin cytoskeleton fully enwrapping the surface of the CAP/CL microparticles. This observation highlights the advantage of therapeutic implantation of nanoparticulate microscopic blocks, rather than dispersed nanoparticles, in terms of (a) enabling the formation of an osteoconductive surface for the thriving of bone-building cells thereon, and (b) exhibiting satisfying drug loading and release profiles, thus contributing to adequate antibacterial performance of the material.

The results of the gene expression analysis of the effects of various CAP/CL powders on osteoblastic MC3T3-E1 cells are displayed in Fig.7. Transcription levels of *BGLAP*, a gene encoding for a protein directly involved in mineralization of the extracellular matrix and a key marker for bone formation, were elevated with respect to the housekeeping gene, *ACTB*, for all CAP/CL powders except MCPM/CL, signifying the mineralization activity of the cells. The expression of all the analyzed osteogenic markers, with the exception of *ALP*, was upregulated with respect to the negative control, suggesting the positive effect of CAP/CL particles on bone formation *in vitro*. Interestingly, DCPA, the most soluble phase that does not induce acidification of the medium below the physiological levels, leads to most drastic upregulation of osteogenic markers compared to the control group: *BSP-1*, *BGLAP*, *Col I*, and *Runx2*. Comparatively high, though still sparse solubility of DCPA led to release of significant amount of phosphate ions, exceeding the critical level of ~ 3 mM according to solubility data and augmenting the fibroblast-to-osteoblast differentiation effect induced by sole AA. In addition, highly bioresorbable DCPA has been shown earlier to promote a more efficient bone healing process upon *in vivo* implantation compared to HAP[37]. This effect may be accounted for by the fact that aside from providing a surface for cells to spread and thrive on, the osteogenic effect of CAP powders comes also from their release of ions constitutive to newly made bone[38,39], the rate of which is higher for DCPA than for ACP and HAP. The only gene whose expression was not consistently upregulated for CAP powders with respect to the control group was *ALP*, which is normal in view of its multiple roles in both differentiated and undifferentiated cells, as well as pathological causes of its elevation[40], aside from that optionally associated with new bone growth.[41] This explains why the only markers found in MCPM cells, fully dead at the time of mRNA collection in the case when the cell growth medium was not replenished after the particles have dissolved, were *ALP*, *Col I*, both of which are common to fibroblasts too, and *BSP-1*. The expression of most analyzed genes in MCPM-incubated cells was markedly lower compared to all other samples, consistent with the lethal effects of the acidification of the medium following its dissolution. The only MCPM gene expression level comparable to the control was *BSP-1*, not surprising since it is known that its upregulation in cells can be a sign of their unviable response to the drug[42] and that it is a negative regulator of proliferation and differentiation in MC3T3-E1 cells[43], coinciding with its role as a mineralization inhibitor[44] rather than promoter, as *BGLAP* or *Col I* are. The absolute expression levels were lowest for *ALP* and *BSP-1*: less than one-fold difference with respect to the housekeeping gene, a sign of cell

viability in view of their augmentation in pathological states. Since *Runx2* is a key transcription factor for osteoblast differentiation[45], the considerable time span of 10 days between mRNA collection and induction of differentiation can explain its comparatively low presence in the cytoplasm.

To decouple the gene regulatory effects of the pure drug from those of CAP carriers, a qPCR analysis was also carried out for each individual component of the composite particles and its results are presented in Fig.8. It is evident that while CL *per se* induces drastic downregulation of osteogenic markers *BGLAP, Col I* and *Runx2*, the gene expression induced by HAP loaded with CL is at the same level as in the presence of pure HAP. Negative effects of pure antibiotics on the activity of osteoblasts *in vitro*, including those of CL in the broad range of concentrations (10 – 500 μg/ml)[46,47], oftentimes similarly reversed upon their incorporation within an osteogenic drug carrier[48], were previously reported.[49–52] These results also shed light on why the two CAP phases with the highest content of the antibiotic and the lowest MICs have led to lower levels of promotion of bone growth markers compared to DCPA with its weaker antibiotic efficacy. A reason for this adverse effect that CL exerts on the cell activity lies in the fact that its dissolution also acidifies the medium to a considerable extent: 1 mg/ml CL solution in the buffered culture media thus yields pH < 7 at room temperature. In these experiments, [CL] = 100 μg/ml was chosen because of its proximity to the previously determined MIC and MBC for growth suppression and eradication of *S aureus*, 25 and 150 μg/ml, respectively. It also lies in the same range as clinically measured levels of gentamicin following its local application[53] as well as in the low range of those of CL released from drug-impregnated polymeric beads.[54] Still, the amount of CL present in CAP powders proved to be sufficiently low not to induce a decrease in cell viability, while effectively eradicating the pathogenic source of infection. These results demonstrate that the osteogenic effect of CAP, the drug carrier, can not only mitigate, but fully reverse the unviable effect that the pure drug has on the cells by ensuring its rather slow release to the environment. The synergy between CAP and CL is thus able to eliminate the negative effects that a sole antibiotic component may exert on its biological milieu, while retaining its antimicrobial potency.

Summary

The multifunctional material developed in this study exerted a satisfactory antibacterial effect against *S aureus*, the main causative agent of osteomyelitis. The most effective phase in this respect was amorphous CAP, owing to its highest drug adsorption efficiency and amorphous surface prone to lattice reorganization via dissolution/recrystallization phenomena, entailing facile release of the surface-bound drug molecules. Coupled with its small molecule drug release time scale of 1–2 months, closest to the duration of the conventional antibiotic therapy for bone infection, amorphous CAP could be potentially favored for the medical application conceived hereby more than any other CAP phase. The microscopic CAP particles loaded with the antibiotic also engaged in an intimate interface with the osteoblastic cells, suggesting their osteoconductive character. All the sparsely soluble antibiotic-loaded CAP powders had a positive morphological effect on cell spreading, while not interfering with the cell viability. They additionally increased osteogenic activity of the osteoblastic cells, as evidenced by their ability to induce upregulation of genes encoding for osteocalcin, type I procollagen and the transcription factor *Runx2*. The most positive effect of monetite, i.e., DCPA, on the expression of osteogenic markers among all CAP powders suggests a direct correlation between (a) the release of constitutive ions from an active surface, particularly phosphates, potent mineralization inductors in MC3T3-E1 cells, and (b) efficacy in compensating for the osteogenic inhibition exerted by the pure antibiotic. The reduced activity of osteoblast-like cells was found to be caused by the antibiotic component of the material, and yet fully

reversed when the drug was released from the sparsely soluble CAP carriers. The simultaneous osteogenic and antimicrobial performance of the material developed in this study, altogether with its ability to exhibit sustained drug release profiles, may favor its consideration as a material base for alternative therapeutic approaches to prolonged antibiotic administration and surgical debridement typically prescribed in the treatment of osteomyelitis.

Supplementary Material

Refer to Web version on PubMed Central for supplementary material.

Acknowledgments

Presented were the results of a study supported by the NIH grant K99-DE021416. The authors would like to thank: Charles Hoover of UCSF for the provision of *S aureus*; Francis Szoka of UCSF for allowing the use of DSC; Feroz Papa lab at UCSF for allowing the use of the qPCR thermocycler; Nikon Imaging Center at UCSF at which confocal microscopy data for this study were acquired.

References

1. Bone Health and Osteoporosis: A Report of the Surgeon General. Rockville, MD: US Department of Health and Human Services, Office of the Surgeon General; 2004.
2. Del Pozo JL, Patel R. Infection Associated with Prosthetic Joints. New Eng J Med. 2009; 361:787–794. [PubMed: 19692690]
3. Hatzenbuehler J, Pulling TJ. Diagnosis and management of osteomyelitis. Am Fam Physician. 2011; 84:1027–1033. [PubMed: 22046943]
4. Kundu B, Nandi SK, Dasgupta S, Datta S, Mukherjee F, Roy S, Singh AK, Mandal TK, Das F, Bhattacharya R, Basu D. Macro-to-micro porous special bioactive glass and ceftriaxone–sulbactam composite drug delivery system for treatment of chronic osteomyelitis: an investigation through in vitro and in vivo animal trial. J Mat Sci Mat Med. 2011; 22:705–720.
5. Waknis V, Jonnalagadda S. Novel poly-DL-lactide-polycaprolactone copolymer based flexible drug delivery system for sustained release of ciprofloxacin. Drug Delivery. 2011; 18:236–245. [PubMed: 21189060]
6. Peng KT, Chen CF, Chu IM, Li YM, Hsu WH, Hsu RW, Chang PJ. Treatment of osteomyelitis with teicoplanin-encapsulated biodegradable thermosensitive hydrogel nanoparticles. Biomat. 2010; 31:5227–5236.
7. El-Ghannam A, Jahed K, Govindaswami M. Resorbable bioactive ceramic for treatment of bone infection. J Biomed Mat Res A. 2010; 94A:308–316.
8. Kanellakopoulou K, Giamarellos-Bourboulis EJ. Carrier systems for the local delivery of antibiotics in bone infections. Drugs. 2000; 59:1223–1232. [PubMed: 10882159]
9. Uskoković V, Uskoković DP. Nanosized hydroxyapatite and other calcium phosphates: Chemistry of formation and application as drug and gene delivery agents. J Biomed Mat Res B. 2011; 96B: 152–191.
10. Dorozhkin SV. Calcium Orthophosphates in Nature, Biology and Medicine. Materials. 2009; 2:399–498.
11. Neto AHC, Machado D, Yano CL, Ferreira CV. Antioxidant defense and apoptotic effectors in ascorbic acid and β-glycerophosphate-induced osteoblastic differentiation. Dev Grow Diff. 2011; 53:88–96.
12. Pfaffl MW. A new mathematical model for relative quantification in real-time RT-PCR. Nucl Acids Res. 2001; 29 45e-45.
13. Guay D. Update on clindamycin in the management of bacterial, fungal and protozoal infections. Exp Opin Pharmacotherapy. 2007; 8:2401–2444.
14. Buffie CG, Jarchum I, Equinda M, Lipuma L, Gobourne A, Viale A, Ubeda C, Xavier J, Pamer EG. Profound Alterations of Intestinal Microbiota following a Single Dose of Clindamycin Results

in Sustained Susceptibility to Clostridium difficile-Induced Colitis. Infect Immun. 2011; 80:62–73. [PubMed: 22006564]

15. Addy LD, Martin MV. Clindamycin and dentistry. BDJ. 2005; 199:23–26. [PubMed: 16003416]
16. Vukomanović M, Škapin SD, Jančar B, Maksin T, Ignjatović N, Uskoković V, Uskoković D. Poly(d,l-lactide-co-glycolide)/hydroxyapatite core-shell nanospheres. Part 1. Coll Surf B. 2011; 82:404–413.
17. Aarts, HJM.; Guerra, B.; Malorny, B. Molecular Methods for Detection of Antibiotic Resistance. In: Aarestrup, FM., editor. Antimicrobial Resistance in Bacteria of Animal Origin. Washington, DC: American Society for Microbiology Press; 2006. p. 55
18. Pace, JL.; Rupp, ME.; Finch, RG. Biofilms, Infection, and Antimicrobial Therapy. Boca Raton, FL: CRC;
19. Quintiliani R, Quintiliani R. Pharmacokinetics for Critical Care Clinicians. Crit Car Cli. 2008; 24:335–348.
20. Kovtun A, Kozlova D, Ganesan K, Biewald C, Seipold N, Gaengler P, Arnold WH, Epple M. Chlorhexidine-loaded calcium phosphate nanoparticles for dental maintenance treatment: combination of mineralising and antibacterial effects. RSC Advances. 2012; 2:870–875.
21. Chalmers G, Kozak GK, Hilyer E, Reid-Smith RJ, Boerlin P. Low minimum inhibitory concentrations associated with the tetracycline-resistance gene tet(C) in E coli. Can J Vet Res. 2010; 74:145–148. [PubMed: 20592845]
22. Reeves DS, Holt HA, Phillips I, King A, Miles RS, Paton R, Wise R, Andrews JM. Activity of clindamycin against S aureus and S epidermidis from four UK centres. J Antim Chemo. 1991; 27:469–474.
23. Gallagher, J.; MacDougall, C. Antibiotics Simplified. Sudbury, MA: Jones and Bartlett Publishers; 2009.
24. Lemaire S, Van Bambeke F, Pierard D, Appelbaum PC, Tulkens PM. Activity of Fusidic Acid Against Extracellular and Intracellular Staphylococcus aureus: Influence of pH and Comparison With Linezolid and Clindamycin. Clinical Infect Diseases. 2011; 52:S493–S503. [PubMed: 21546626]
25. Connors, KA.; Amidon, GL.; Stella, VJ. Chemical Stability of Pharmaceuticals. Hoboken, NJ: Wiley; 1986.
26. Weinrick B, Dunman PM, McAleese F, Murphy E, Projan SJ, Fang Y, Novick RP. Effect of Mild Acid on Gene Expression in Staphylococcus aureus. J Bacteriology. 2004; 186:8407–8423.
27. Baudoux P, Bles N, Lemaire S, Mingeot-Leclercq MP, Tulkens PM, Van Bambeke F. Combined effect of pH and concentration on the activities of gentamicin and oxacillin against Staphylococcus aureus in pharmacodynamic models of extracellular and intracellular infections. J Antimicr Chem. 2006; 59:246–253.
28. Morozowich W, Karnes HA. Case Study: Clindamycin 2-Phosphate. Biotech: Pharm Asp. 2007; 5:1207–1219.
29. Iafisco M, Palazzo B, Martra G, Margiotta N, Piccinonna S, Natile G, Gandin V, Marzano C, Roveri N. Nanocrystalline carbonate-apatites: role of Ca/P ratio on the upload and release of anticancer platinum bisphosphonates. Nanoscale. 2012; 4:206–217. [PubMed: 22075933]
30. Johnson ML, Uhrich KE. Concurrent release of admixed antimicrobials and salicylic acid from salicylate-based poly(anhydride-esters). J Biomed Mat Res A. 2009; 91A:671–678.
31. Gelperina S, Kisich K, Iseman MD, Heifets L. The Potential Advantages of Nanoparticle Drug Delivery Systems in Chemotherapy of Tuberculosis. Am J Resp Crit Care Med. 2005; 172:1487–1490. [PubMed: 16151040]
32. Radi S, Ducheyne P. Nanostructural Control of Implantabale Xerogels for the Controlled Release of Biomolecules. NATO Sci Series II: Math Phys Chem. 2004; 171:59–74.
33. Mourino V, Boccaccini AR. Bone tissue engineering therapeutics: controlled drug delivery in three-dimensional scaffolds. J Royal Soc Interface. 2009; 7:209–227.
34. Vukomanović M, Škapin SD, Poljanšek I, Zagar E, Kralj B, Ignjatović N, Uskoković D. Poly(D,L-lactide-co-glycolide)/hydroxyapatite core-shell nanosphere. Part 2. Coll Surf B. 2011; 82:414–421.

35. Cameron DR, Howden BP, Peleg AY. The interface between antibiotic resistance and virulence in Staphylococcus aureus and its impact upon clinical outcomes. Clin Infect Dis. 2011; 53:576–582. [PubMed: 21865195]
36. Pigrau C, Almirante B, Rodriguez D, Larrosa N, Raspall G, Pahissa A. Osteomyelitis of the jaw: resistance to clindamycin in patients with prior antibiotics exposure. Eur J Clin Micr Inf Dis. 2008; 28:317–323.
37. Tamimi F, Torres J, Bassett D, Barralet J, Cabarcos EL. Resorption of monetite granules in alveolar bone defects in human patients. Biomat. 2010; 31:2762–2769.
38. An S, Ling J, Gao Y, Xiao Y. Effects of varied ionic Ca and PO_4 on the proliferation, osteogenic differentiation and mineralization of human periodontal ligament cells. J Perio Res. 2012; 47:374–382.
39. Varanasi VG, Owyoung JB, Saiz E, Marshall SJ, Marshall GW, Loomer PM. The ionic products of bioactive glass particle dissolution enhance periodontal ligament fibroblast osteocalcin expression and enhance early mineralized tissue development. J Biomed Mat Res A. 2011; 98A:177–184.
40. Bramer JAM, van Linge JH, Grimer RJ, Scholten RJPM. Prognostic factors in localized extremity osteosarcoma: A systematic review. Eur J Surg Oncology. 2009; 235:1030–1036.
41. Xu L, Lv K, Zhang W, Zhang X, Jiang X, Zhang F. The healing of critical-size calvarial bone defects in rat with rhPDGF-BB, BMSCs, and β-TCP scaffolds. J Mater Sci Mater Med. 2012; 23:1073–1084. [PubMed: 22311076]
42. Sakamoto W, Isomura H, Fujie K, Deyama Y, Kato A, Nishihira J, Izumi H. Homocysteine attenuates the expression of osteocalcin but enhances osteopontin in MC3T3-E1 preosteoblastic cells. Biochim Biophys Acta. 2005; 1740:12–16. [PubMed: 15878736]
43. Huang W, Carlsen B, Rudkin G, Berry M, Ishida K, Yamaguchi DT, Miller TA. Osteopontin is a negative regulator of proliferation and differentiation in MC3T3-E1 pre-osteoblastic cells. Bone. 2004; 34:799–808. [PubMed: 15121011]
44. Sodek J, Ganss B, McKee MD. Osteopontin. Crit Rev Oral Biol Med. 2000; 11:279–303. [PubMed: 11021631]
45. Carbonare LD, Innamorati G, Valenti MT. Transcription Factor Runx2 and its Application to Bone Tissue Engineering. Stem Cell Rev. 2012 in press.
46. Naal FD, Salzmann GM, von Knoch F, Tuebel J, Diehl P, Gradinger R, Schauwecker J. The effects of clindamycin on human osteoblasts in vitro. Arch Orthop Trauma Surgery. 2008; 128:317–323.
47. Duewelhenke N, Krut O, Eysel P. Influence on Mitochondria and Cytotoxicity of Different Antibiotics Administered in High Concentrations on Primary Human Osteoblasts and Cell Lines. Antimicrob Agent Chemotherapy. 2006; 51:54–63.
48. Ince A, Schütze N, Hendrich C, Thull R, Eulert J, Löhr JF. In vitro investigation of orthopedic titanium-coated and brushite-coated surfaces using human osteoblasts in the presence of gentamycin. J Arthropl. 2008; 23:762–771.
49. Antoci V, Adams CS, Hickok NJ, Shapiro IM, Parvizi J. Antibiotics for Local Delivery Systems Cause Skeletal Cell Toxicity In Vitro. Clin Orthop Relat Res. 2007; 462:200–206. [PubMed: 17572634]
50. Holtom PD, Pavkovic SA, Bravos PD, Patzakis MJ, Shepherd LE, Frenkel B. Inhibitory effects of the quinolone antibiotics trovafloxacin, ciprofloxacin, and levofloxacin on osteoblastic cells in vitro. J Orthop Res. 2000; 18:721–727. [PubMed: 11117292]
51. Almazin SM, Dziak R, Andreana S, Ciancio SG. The Effect of Doxycycline Hyclate, Chlorhexidine Gluconate, and Minocycline Hydrochloride on Osteoblastic Proliferation and Differentiation In Vitro. J Periodont. 2009; 80:999–1005. [PubMed: 19485832]
52. Ince A, Schütze N, Hendrich C, Thull R, Eulert J, Löhr JF. Effect of polyhexanide and gentamycin on human osteoblasts and endothelial cells. Swiss Med Wkly. 2007; 137:139–145. [PubMed: 17370154]
53. Isefuku S, Joyner CJ, Simpson AHRW. Gentamicin May Have an Adverse Effect on Osteogenesis. J Orthop Trauma. 2003; 17:212–216. [PubMed: 12621263]
54. Adams K, Couch L, Cierny G, Calhoun J, Mader JT. In vitro and in vivo evaluation of antibiotic diffusion for antibiotic-impregnated polymethylmethacrylate beads. Clin Orthop. 1992; 278:244–252. [PubMed: 1563160]

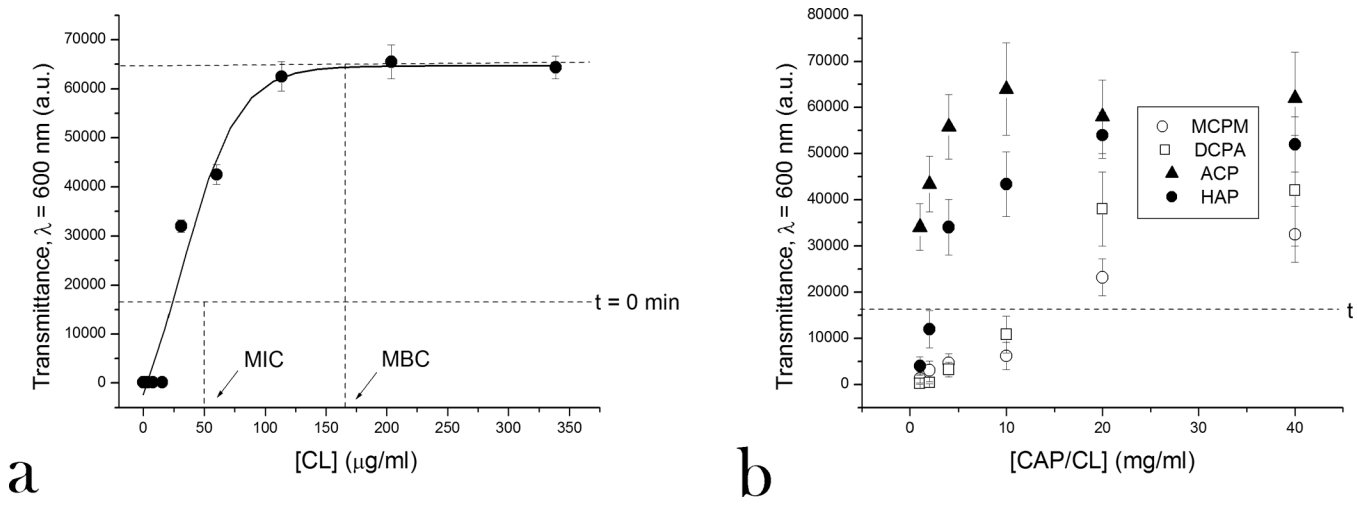

Fig.1.

Optical transparence at λ = 600 nm of BHI broths inoculated with *S aureus* (10^5 bacteria per ml) and different amounts of CL (a) and different CAP phases loaded with CL (b), following 24 h incubation.

Fig. 2.
Averaged color of pure CL, pure ACP and different CAP powders loaded with CL after their annealing to 200 °C in air, at the heating rate of 10 °C/min.

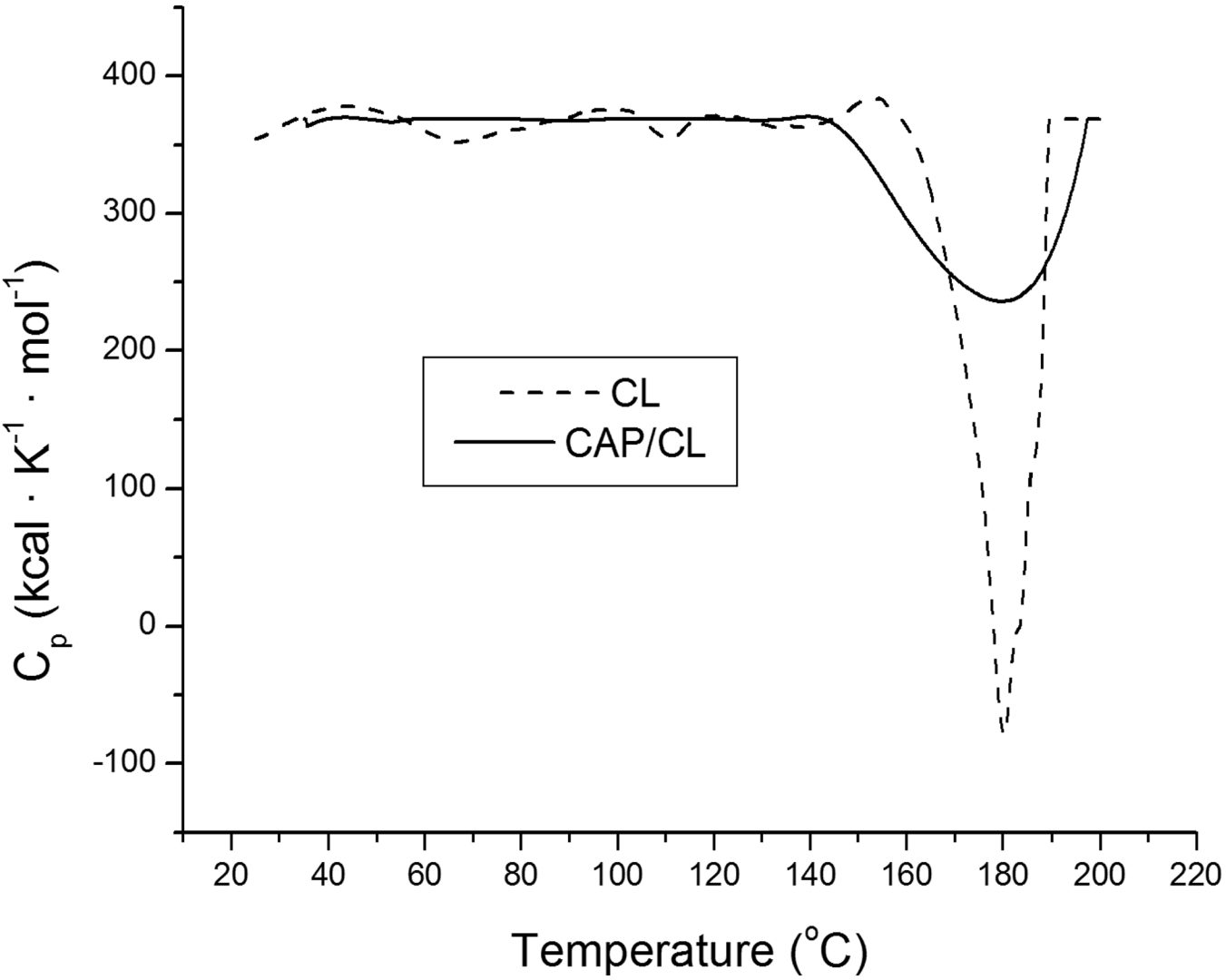

Fig.3.
DSC diagrams of pure CL (dashed line) and CL encapsulated within DCPA powder (straight line).

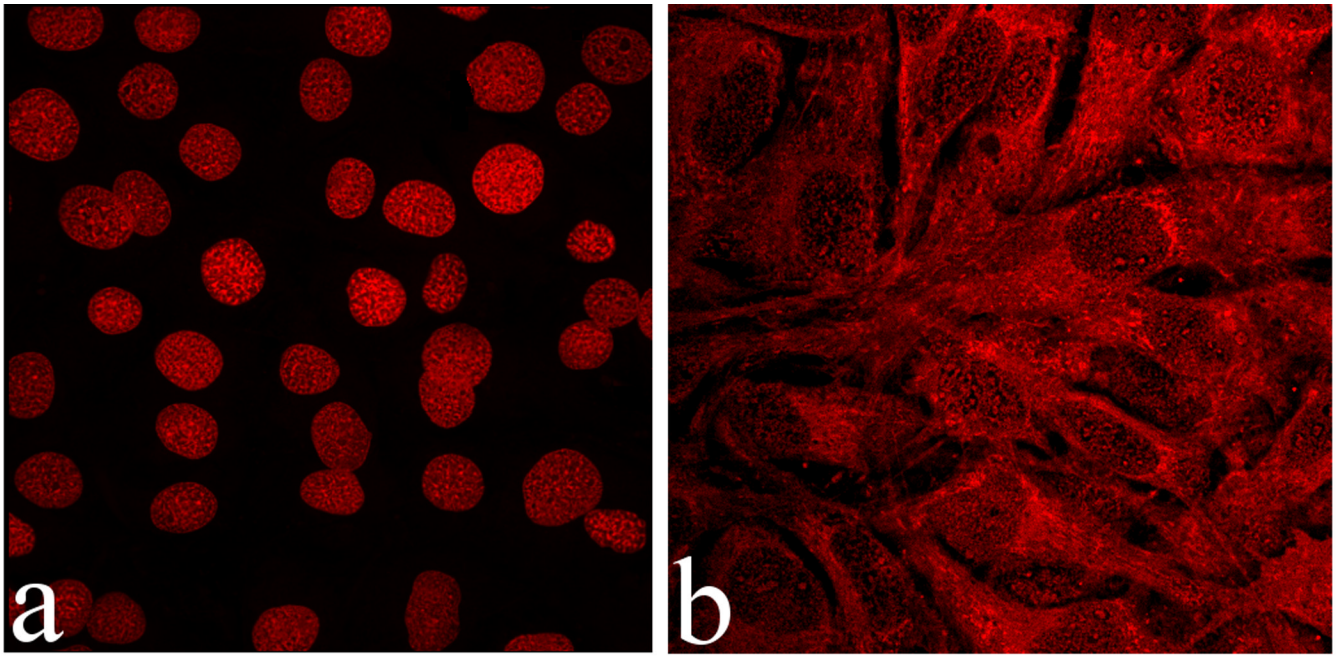

Fig.4.

Single plane confocal optical micrographs of fluorescently stained osteoblastic MC3T3-E1 cells following 7 days of incubation with MCPM/CL, in cases when the cell growth medium was replenished 48 h after the addition of the particles (a) and immediately upon their dissolution and drug release (1 – 2 h) (b); The sizes of the images are 450×450 μm (a) or 270×270 μm (b).

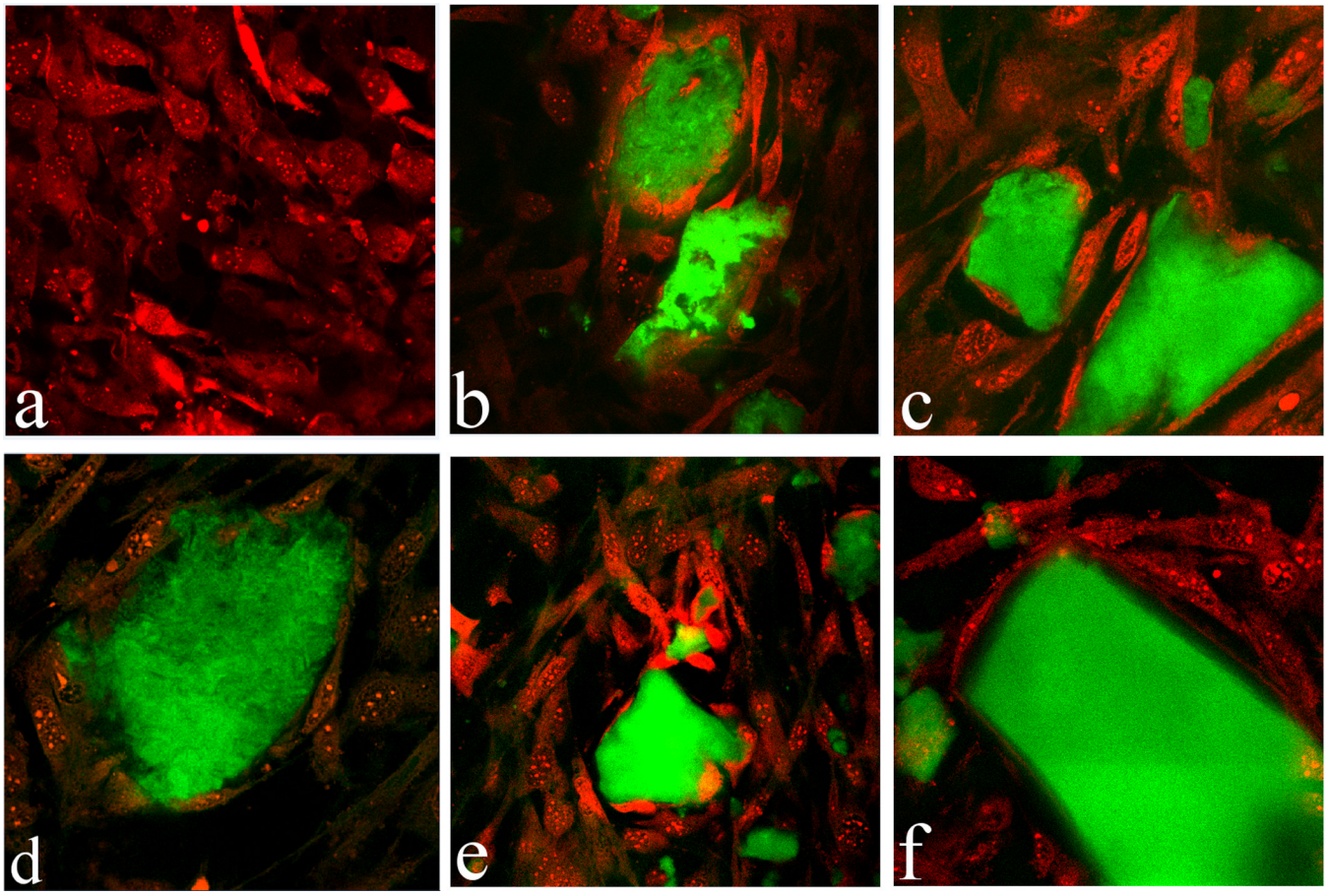

Fig.5.
Single plane confocal optical micrographs of fluorescently stained CAP/CL particles (green) and osteoblastic MC3T3-E1 cells (red) following 7 days of incubation in differentiation medium: (a) control; (b) HAP/CL; (c, d) ACP/CL; (e, f) DCPA/CL; The sizes of the images are 450×450 μm (a, b, d, e) or 270×270 μm (c, f).

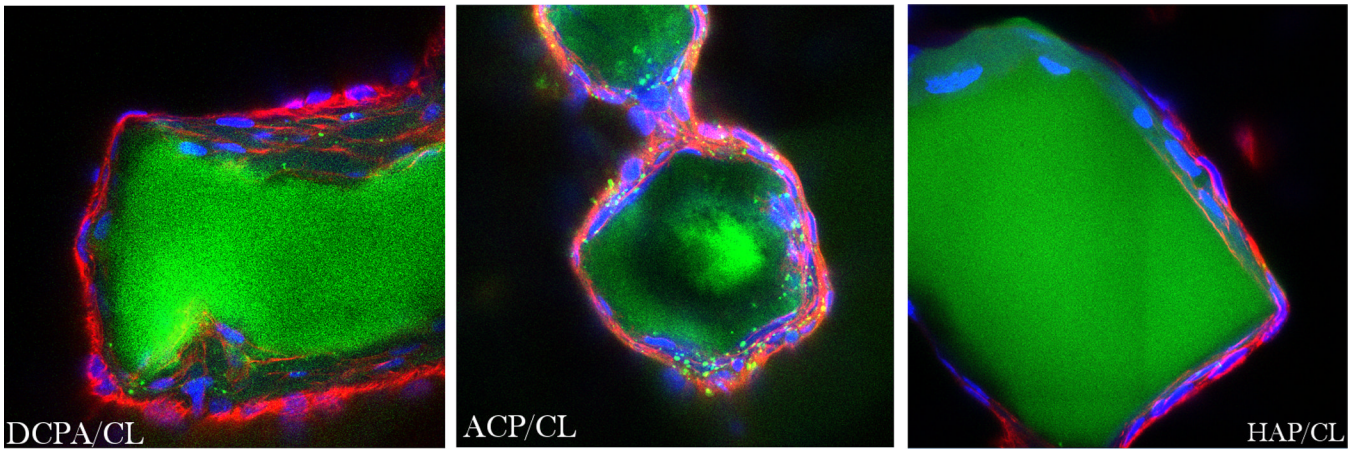

Fig.6.

Single plane confocal optical micrographs of fluorescently stained DCPA/CL, ACP/CL and HAP/CL particles (green) and osteoblastic MC3T3-E1 cells (cytoskeletal f-actin - red; nucleus - blue) following 7 days of incubation in differentiation medium. The sizes of the images are 270×270 μm.

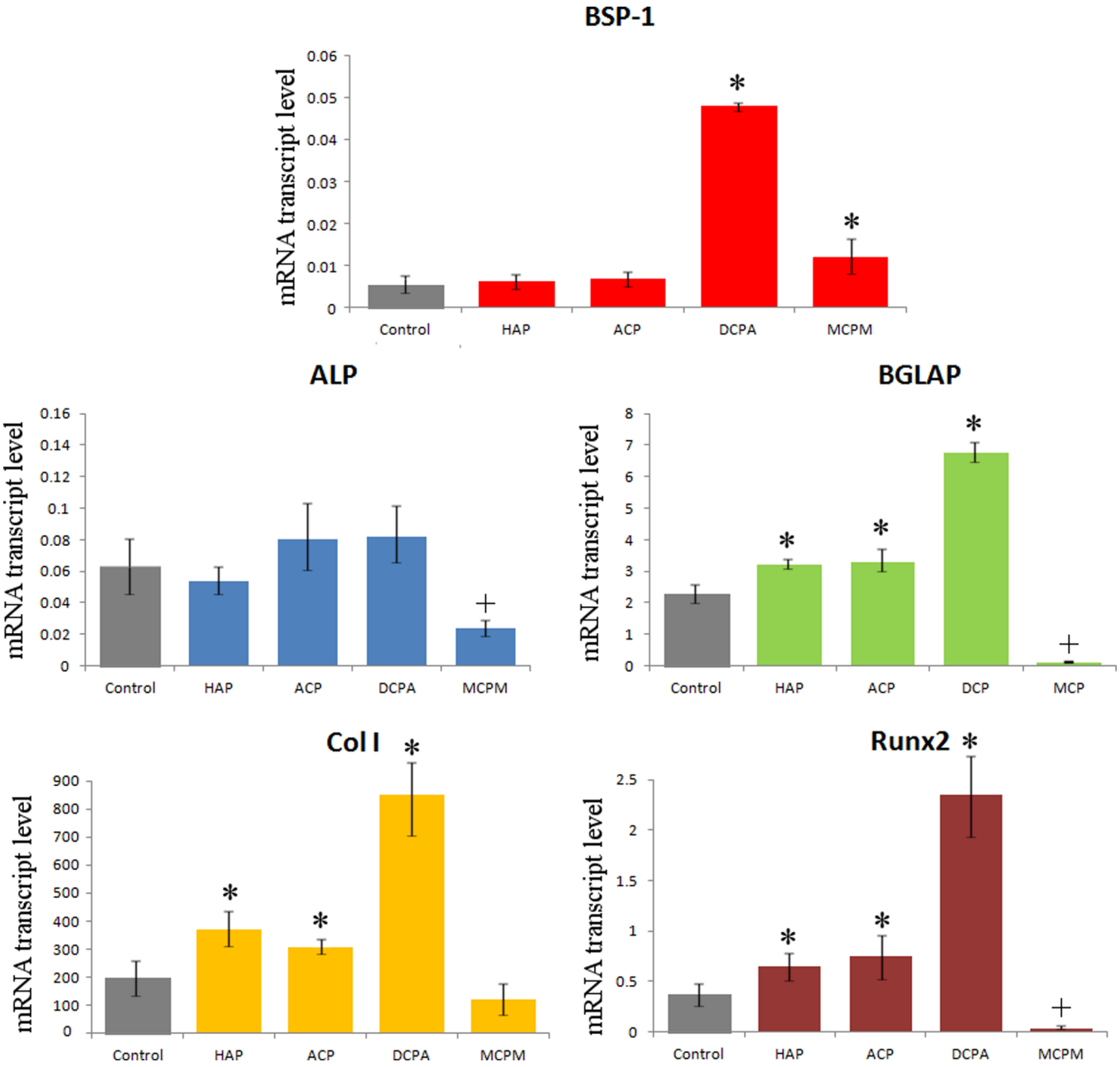

Fig.7.

The effect of CAP particles loaded with CL on the mRNA expression of five different osteogenic markers: *BSP-1*, *ALP*, *BGLAP*, *Col I* and *Runx2* in osteoblastic MC3T3-E1 cells. mRNA expression was detected by quantitative RT-polymerase chain reaction relative to the housekeeping gene *ACTB*. Data normalized to expression of *ACTB* are shown as averages with error bars representing standard deviation. Genes significantly ($p < 0.05$) upregulated with respect to the control group are marked with *. Genes significantly ($p < 0.05$) downregulated with respect to the control group are marked with $^{+}$.

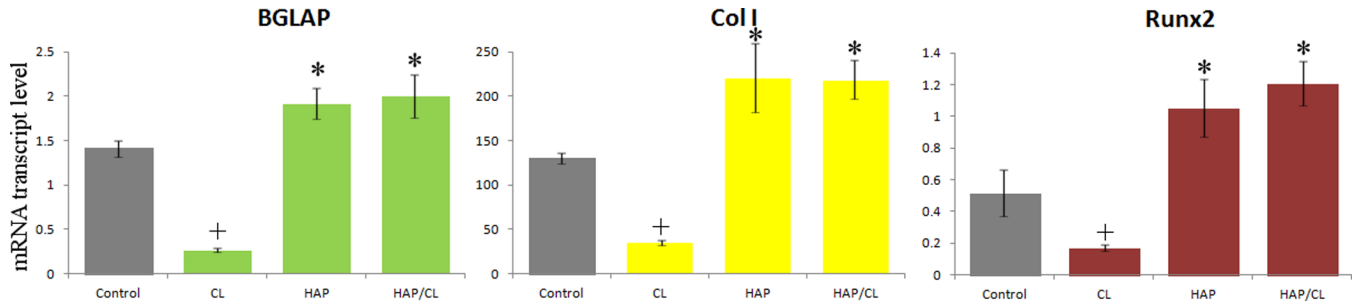

Fig.8.

The effect of pure CL, pure HAP and HAP loaded with CL on the mRNA expression of three different osteogenic markers: *BGLAP*, *Col I* and *Runx2* in osteoblastic MC3T3-E1 cells. mRNA expression was detected by quantitative RT-polymerase chain reaction relative to the housekeeping gene *ACTB*. Data normalized to expression of *ACTB* are shown as averages with error bars representing standard deviation. Genes significantly ($p < 0.05$) upregulated with respect to the control group are marked with *. Genes significantly ($p < 0.05$) downregulated with respect to the control group are marked with $^{+}$.

Table 1

CAP phases synthesized as a part of this study.

Phase	Chemical formula	Space group	pK_{sp} at 37 °C	Ca/P molar ratio
MCPM *	$Ca(H_2PO_4)_2{\cdot}H_2O$	Triclinic $P\bar{1}$	1.14	0.5
DCPA *	$CaHPO_4$	Triclinic $P\bar{1}$	7.0	1
β-CPP *	$Ca_2P_2O_7$	Tetragonal $P4_1$	18.5	1
ACP *	$Ca_3(PO_4)_2{\cdot}nH_2O$	/	25	1.3–1.5
HAP *	$Ca_{10}(PO_4)_6(OH)_2$	Pseudo-Hexagonal $P6_3/m$	117.3	1.67

* MCPM = monocalcium phosphate monohydrate; DCPA = dicalcium phosphate anhydrous; CPP = calcium pyrophosphate; ACP = amorphous calcium phosphate (data pertain to the phase obtainable at pH 9 – 11)[10]; HAP = hydroxyapatite.

Table 2

MIC values and drug percentage for different CAP powders loaded with CL.

CAP phase	MIC (mg/ml)	Estimated effective content of CL in CAP/CL (wt%)
HAP	2.5	3
ACP	< 1	> 5
DCPA	12	0.8
MCPM	15	0.2